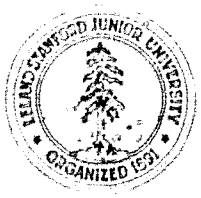

Department of AERONAUTICS and ASTRONAUTICS
STANFORD UNIVERSITY

Semi-Annual Progress Report

July 1, 1980 - December 31, 1980

on

DENSITY MEASUREMENT IN AIR WITH A SATURABLE ABSORBING SEED GAS

NASA-Ames Grant No. NAG 2-36

Submitted to the

National Aeronautics and Space Administration

Ames Research Center

Moffett Field, California 94035

R.L. McKenzie - Technical Officer

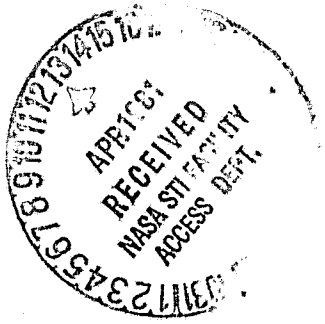

by the

Department of Aeronautics and Astronautics

Stanford University

Stanford, California

Principal Investigator

Donald Baganoff

March 1981

ABSTRACT

Resonantly-enhanced scattering from the iodine molecule is studied, experimentally, for the purpose of developing a scheme for the measurement of density in a gas dynamic flow. A study of the spectrum of iodine, the collection of saturation data in iodine, and the development of a mathematical model for correlating saturation effects were pursued for a mixture of 0.3 torr iodine in nitrogen and for mixture pressures up to one atmosphere. For the pressure range of interest in gas dynamic studies, saturation effects in iodine were found to be too small to be useful in allowing density measurements to be made. The reason the effects are too small in iodine is that iodine predissociates quite readily from its excited state and thereby alters the excited state population, an effect not removed by saturation. At the cost of lower signal intensity (compared with fluorescence), effects of quenching can be reduced by detuning the exciting laser wavelength from the absorption line center of the iodine line used (resonant Raman scattering). The signal was found to be nearly independent of pressure, for pressures up to one atmosphere, when the excitation beam was detuned 6 GHz from line center for an isolated line in iodine. The signal amplitude was found to be nearly equal to the amplitude for fluorescence at atmospheric pressure, which indicates a density measurement scheme is possible using resonant Raman scattering in iodine.

1. INTRODUCTION

The objective of this work is to study the application of the principle of saturation in absorbing and radiating molecular systems to the development of a scheme for measuring gas density in a nonsteady gas dynamic flow. At the time the proposal was funded (July 1980) we were actively studying the saturation properties of iodine as a candidate seed gas. This was an outgrowth of our earlier work with sulfur hexafluoride which we were pursuing at the time the proposal was originally submitted (December 1978). Iodine became the more interesting gas for exploring the method because it absorbs and radiates in the visible part of the spectrum where various optical detectors and devices are more readily available (as opposed to the infrared for sulfur hexafluoride) and it was agreed that the study with iodine should be continued.

Iodine has been thoroughly studied at very low pressures and it is well known that it actively absorbs the 514.5 nm Argon-ion laser line and has a rather strong fluorescence in the orange-red part of the spectrum. In our work we observed that its fluorescence was not entirely quenched at atmospheric conditions and therefore it had potential utility as a seed gas in a gas dynamic situation. Because of its low saturation intensity (approximately 10^4 Watts/cm^2) at very low pressures, a number of fundamental experiments, having potential application to density measurements, have been conducted with iodine by various researchers by making use of its saturated state.

The approach we were interested in exploring was to determine if iodine could be saturated in fluorescence at higher pressures (using a

buffer gas of nitrogen or air) so that its fluorescence would be independent of pressure and depend only on the concentration of iodine present in the gas mixture. The fluorescence intensity would therefore be directly related to the local density in the flow of a premixed gas.

One direction the study has taken was guided by the following simple analysis. Consider a test cell filled with a known mixture of iodine vapor and nitrogen gas at a given temperature and pressure and let the gas mixture be excited by resonant laser radiation. In a very general way, one can express the steady-state intensity of the fluorescent signal, S, as a function of four variables:

$$S = S([I_2], [N_2], T, I) ,$$

where $[I_2]$ and $[N_2]$ are the concentrations of iodine and nitrogen, respectively, T is the temperature, and I is the laser intensity. In a gas dynamic situation where the density changes are small (five per cent or less), one may differentiate the above equation and write

$$dS = \frac{\partial S}{\partial [I_2]} d[I_2] + \frac{\partial S}{\partial [N_2]} d[N_2] + \frac{\partial S}{\partial T} dT + \frac{\partial S}{\partial I} dI .$$

The last term on the right-hand side can be made zero by running the experiment at constant laser intensity. If the iodine concentration is very small, the general expression for S reduces to a product of $[I_2]$ and some function of $[N_2]$ and T, that is

$$S = [I_2] F([N_2], T) .$$

On this basis, we have

$$\frac{\partial S}{\partial [I_2]} = \frac{S}{[I_2]} .$$

In addition, for density fluctuations in a premixed flow, we can employ the substitution

$$d[I_2]/[I_2] = d[N_2]/[N_2] = d\rho/\rho \ ,$$

where ρ is the density of the gas mixture. Finally, we can express our equation for dS in the dimensionless form

$$\frac{dS}{S} = \frac{d\rho}{\rho} + \left[\frac{\rho}{S} \frac{\partial S}{\partial \rho} \right] \frac{d\rho}{\rho} + \left[\frac{T}{S} \frac{\partial S}{\partial T} \right] \frac{dT}{T} \quad . \tag{1}$$

The first term on the right-hand side of (1) gives the desired direct relation between changes in gas density and changes in fluorescence intensity. This term results from the change in iodine concentration as the gas mixture is compressed. The second term can be shown to be principally related to the increase in the quenching rate with an increase in nitrogen density. Because the partial derivatives appearing in (1) are evaluated while holding the other variables held fixed, the third term represents the effect of the increase in the quenching rate with increasing gas temperature. Because quenching decreases fluorescence intensity, the last two terms on the right-hand side are expected to be negative. Unfortunately, in most situations the negative contributions nearly balance the first term and a detection scheme for measuring gas density based on fluorescence results in very poor sensitivity. On the other hand, if one were able to fully saturate iodine and eliminate the last two terms altogether, one would then obtain the ideal sensititity $dS/S = d\rho/\rho$. For the case of partial saturation, one can again express equation (1) in terms of $d\rho/\rho$ if one assumes the small disturbances occur in an isentropic flow where one

may use the substution $dT/T = 0.4\ d\rho/\rho$ (for $\gamma = 1.4$). Equation (1) then becomes:

$$\frac{dS}{S} = \left[1 + \frac{\rho}{S}\frac{\partial S}{\partial \rho} + 0.4\,\frac{T}{S}\frac{\partial S}{\partial T} \right] \frac{d\rho}{\rho}\ , \qquad (2)$$

where each term in the square braces is evaluated at the unperturbed or reference state.

The first partial derivative can be obtained experimentally by measuring the slope of the curve exhibiting fluorescence intensity versus gas density (or pressure) for a fixed gas temperature and laser intensity. The second partial derivative can be obtained in a similar way by varying the gas temperature while holding the density and laser intensity fixed.

Most of our work to date has been directed towards a study of the spectrum of iodine fluorescence, a mathematical model for correlating saturation effects in iodine, and a measurement of the first partial derivative in equation (2).

2. HIGH-PRESSURE SPECTRUM OF IODINE

The visible absorption spectrum of iodine results from transitions in the electronic structure of the molecule from the ground state, $X^1\Sigma_g^+$, to the excited state $B^3\pi_u^+$. Potential energy curves of the X and B states for molecular iodine, together with the curve of the dissociative D state (which was found to be needed in modeling iodine saturation), are shown in Fig. 1.

The B←X transition is between states of different electronic spin and is thus weakly allowed. For this reason the radiative lifetime of the B state is relatively long ($\sim 10^{-6}$ sec) compared to a typical radiative lifetime at this wavelength of 10^{-8} sec for most other gases.

Absorption can occur from any populated ground state rotation-vibrational level to an excited state level allowed by the selection rules and with strength determined by the overlap of the vibrational wavefunctions (Frank-Condon factors). The selection rule on J is $\Delta J = \pm 1$ for a homonuclear diatomic molecule and, thus, each transition is made up of a P ($\Delta J = -1$) and R ($\Delta J = +1$) component. At room temperature there are about 150 rotational levels populated, each giving a P and R absorption line. With population at room temperature in $v'' = 0$, 1, and 2 and about 80 vibrational levels available for transitions in the B state, this produces about 70,000 absorption lines in the visible (500 - 700 nm) B←X spectrum. The density of the spectrum derives from the closely spaced vibrational and rotational energy levels for this relatively massive molecule.

At room temperature, the absorption lines are Doppler broadened by an amount $\Delta_{\text{Doppler}} \approx 440$ MHz at the 514.5 nm Argon-ion laser wavelength.

In a sub-Doppler absorption spectrum, it is seen that each even J sublevel is further split into 15 hyperfine components and each odd sublevel into 21, due to the interaction of the total nuclear spin and rotational angular momentum.

For each v' level populated by absorption, a vibrational progression (v'' ← v') of fluorescence bands will occur with strengths determined by the Frank-Condon factors. Each J' value gives rise to a P and R fluorescence doublet spaced by about 1 cm^{-1}. The fluorescence spectrum is thus very complicated if several vibrational-rotational levels are populated in the excited state.

Within the 6 GHz Argon-ion laser gain profile (tuning range) lies two v'' = 0 transitions and two hot-band transitions, as seen in Fig. 2. The strong line is composed of the overlapping P13 and R15 absorption lines of the 43←0 vibrational transition (shown schematically in Fig. 3). The P13 and R15 lines each have 21 hyperfine components spread over about 1.2 GHz. Adding the room temperature Doppler width of each component gives an overall linewidth of about 1.5 GHz (FWHM). Each component also pressure broadens at about 3 MHz/torr, giving a total linewidth of about 4 GHz at 1 atmosphere of pressure (nitrogen).

The low-pressure fluorescence spectrum due to pumping of the 43←0 lines contains a progression of v'' ← v' bands, spaced by the ground state vibrational spacing. Figure 4 shows the progression through the 5th Stokes component obtained with a low-pressure iodine cell and excitation by the 514.5 nm laser wavelength. (The cell was at room temperature and contained approximately 0.3 torr iodine, the vapor pressure of iodine at this temperature.) Each Stokes component under higher resolution appears

to be a triplet. Figure 5 shows the triplet of the 2nd stokes component at 526 nm. As seen in Fig. 3, there are actually four rotational components to each $v'' \leftarrow v'$ band but the P13 and R15 overlap to within the resolution of the spectrometer.

The effect on the spectrum of adding nitrogen at various pressures to the iodine cell is seen in Fig. 6. As the pressure increases, collisions transfer population to adjacent rotational then vibrational levels in the excited state which then fluoresce, giving rise to the so-called transfer spectrum. The ratio of transfer to primary fluorescence increases until at a pressure of 500 torr (nitrogen) the primary progression is almost lost in the transfer spectrum.

This figures clearly shows that once the pressure is 100 torr or greater one must collect broadband fluorescence because the Stokes components of the primary band are obscured by the transfer spectrum. Likewise, owing to the pressure broadening of iodine, it is probably best to operate the Argon-ion laser in the broadband mode in order to maximize the fluorescence signal.

3. SATURATION OF IODINE FLUORESCENCE

Iodine is an attractive molecule to attempt to saturate because its absorption cross-section is relatively large ($\sim 5 \times 10^{-17}$ cm^2) and its lifetime long. The saturation intensity is estimated to be 8×10^3 Watts/cm^2 at low pressure and 1.9×10^6 Watts/cm^2 in a mixture of 0.3 torr iodine and 800 torr nitrogen. Focused CW Argon-ion laser power densities of 10^7 W/cm^2 are readily obtained, making saturation near atmospheric pressure seem reasonable. Compared to a molecule like biacetyl, with a cross-section of $\sim 10^{-19}$ cm^2 and a radiative lifetime of $\sim 10^{-8}$ sec, the saturation intensity for iodine is about four orders of magnitude lower.

Data were collected for the saturation experiment in iodine using the setup shown in Fig. 7. The Argon-ion laser supplied about 3.4 Watts running multimode over about 6 GHz at 514.5 nm. The beam was aperatured so as to be nearly Gaussian (TEM_{00}) and focused to a 6 μm spot size (measured with a reticon array) by a 5.1 cm focusing lens. Crossed Glan-air polarizers gave a $\cos^4\theta$ attenuation over about five orders of magnitude with no observable beam steering. A cell containing iodine crystals was placed at the beam focus and connected to a gas handling system for adding N_2. A thermocouple placed on the cell monitored the cell-crystal temperature. The fluorescence was collected at 90° with an 8-cm focal length lens and focused through an aperature (allowing monitoring of one confocal parameter length of the beam at the focus) and a 540 nm long pass filter (to block scattered 514.5 nm radiation) onto a photocathode. The beam was chopped and the fluorescence signal collected using phase sensitive detection, yielding a background siganl (no iodine in cell) near the noise

level of the photomultiplier tube. The iodine crystals remained at about 25°C producing a room temperature vapor pressure of about 0.3 torr. Some problems were encountered with the cell due to room temperature drifts and heating by the laser beam (both producing changes in iodine vapor pressure). However, with much care, consistent and repeatable data were obtained. Most of the data were collected with the Argon-ion laser running multimode.

Tests were conducted for buffer-gas pressures (nitrogen) of 0.9, 50, 100, 200, 400, 600, and 800 torr and these results are shown in Figs. 8 through 14. Complete saturation was not achieved even though the fluorescence signal versus laser intensity became nonlinear well below the maximum intensity used (about 2×10^6 Watts/cm^2). A measure of the degree of saturation achieved is given by the second slope at high laser intensities shown in each figure. Complete saturation, of course, is obtained once this slope becomes zero.

In reviewing and analyzing the data to understand the reason for its behavior, Daily's saturation model[3] was studied and its application to iodine considered. His two-level model leads to the following expression for the fluorescence signal

$$S = h\nu \frac{A_{21}}{4\pi} \Omega_c V_c \beta N_T [I_\nu/(I_\nu + I_\nu^s)] \ , \qquad (3)$$

where A_{21} is the Einstein coefficient for spontaneous emission from level 2 to level 1, Ω_c the collection solid angle, V_c the sample volume, N_T the total iodine number density (levels 1 and 2), β a constant given by

$$\beta = 1/(1 + g_1/g_2) \ ,$$

and I_ν^s the saturation intensity (per unit bandwidth) given by

$$I_\nu^s = (Q_{21} + A_{21})/B_{12}(1 + g_1/g_2) ,$$

where Q_{21} is the quenching rate, B_{12} the stimulated emission rate, and g_i the statistical weights.

In the low intensity limit ($I_\nu << I_\nu^s$) and for buffer gas pressure near one atmosphere where $Q_{21} >> A_{21}$, the fluorescence signal becomes

$$S = h\nu \frac{A_{21}}{4\pi} \Omega_c V_c B_{12} (N_T/Q_{21}) I_\nu . \tag{4}$$

In this limit the signal varies linearly with laser intensity but it is completely insensitive to gas density because the ratio N_T/Q_{21} is independent of the total density (in the premixed situation). This is consistent with the discussion following (1).

Likewise, in the high intensity limit ($I_\nu >> I_\nu^s$), the fluorescence signal becomes independent of laser intensity and quenching rates and depends linearly on the iodine density throught the term N_T:

$$S = h\nu \frac{A_{21}}{4\pi} \Omega_c V_c \beta N_T . \tag{5}$$

Equation (5) provides the motivation for seeking a saturable process because it would lead to a direct method for measuring density which is, coincidently, independent of laser intensity. Also, if the conditions of (5) could be realized, the measurement would be precise because the coefficients appearing in (5) are truly constant.

The data presented in Figs. 8 through 14 agree with (4) rather well because each slope at the low intensity end is near unity, but clearly (5) is not realized at the high intensity end because the fluorescence signal

is not independent of laser intensity or buffer gas pressure. A number of nonideal effects are clearly indicated by the data and several of these have been considered in studying the results we have obtained.

The laser used to excite the fluorescence is expected to have a Gaussian intensity distribution over its cross-section, rather than a constant intensity as assumed in the derivation of equation (3). Daily has considered this effect and placed the Gaussian distribution in the expression for the excited state population and integrated over a cylindrical sampling volume of width δ to obtain

$$S = h\nu \frac{A_{21}}{4\pi} \Omega_c \delta \beta N_T \pi \omega^2 \ln[(I_\nu^o + I_\nu^s)/I_\nu^s] \quad . \tag{6}$$

where I_ν^o is the intensity on the center line of the laser beam and ω is its halfwidth. Equation (6) predicts that the intensity will not saturate at any power level because the molecules in the wings of the laser beam are in a region of low intensity and will never be fully saturated.

Daily's saturation models assume that the laser linewidth is much greater than the molecular linewidth and, therefore, the details of the molecular lineshape are not important. The laser intensity is also assumed to be constant across the transition. This leads to a homogeneous saturation model of the usual type

$$S \sim I_\nu/(I_\nu + I_\nu^s) \quad .$$

Actually, three linewidths must be considered: the Lorentzian (homogeneous or pressure broadened) linewidth, the Doppler (inhomogeneous or temperature dependent) linewidth, and the laser linewidth. The relative contributions of the first two determine the lineshape of the transition.

For the case where the laser linewidth is not small with respect to the molecular linewidth, Greenstein[4] has shown that the homogeneous width is determined by both the laser and the Lorentzian widths and, thus, the laser bandwidth would make the transition appear homogeneous even if the Doppler width is greater than the Lorentzian width. Although this case is consistent with Daily's model, Killinger et al.[5] have shown that the fluorescence of OH at low pressures (transition inhomogeneously broadened) saturates with a residual slope of 0.5 when they used a broadband laser with discrete oscillating modes. In the limit of an inhomogeneously broadened transition the saturation is described by

$$S \sim \tilde{I}/(1 + \tilde{I})^{0.5} \qquad \text{where} \qquad \tilde{I} = I_\nu / I_\nu^s \ .$$

Since the broadband Argon-ion laser output contains about 60 oscillating modes, it is expected that the model should include the possibility of inhomogeneous lineshape in the case of Doppler width $\gtrsim$ Lorentzian width. (In the case of homogeneous lineshape the laser linewidth should not be important.)

Finally, the two-level model may be an oversimplification of the situation in iodine. If other levels are tightly coupled to the two resonance levels then they must be included in the rate equation model used to calculate the population of the upper state, N_2. Daily showed that in this case the factor β is given by

$$\beta = \left[1 + \frac{g_i}{g_k} + \sum_{i \neq k} (N_i/N_k)^* \right]^{-1} = \beta(Q_{ki}) \ ,$$

where the quasi-equilibrium population ratios of nonresonant levels

involve the quenching rates. The expression for the saturation intensity is also different. The nonresonant levels siphon population from the resonant levels, reducing the fluorescence signal and, possibly, affecting the saturation intensity. The important point to be made is that even in the case of complete saturation, the fluorescence signal still depends on Q_{ki} through the factor β. Full saturation would eliminate laser intensity dependence but not the quenching complication.

The following analysis was carried out to attempt to address some of the nonideal effects discussed above and to build a theory that is consistent with the data obtained for iodine. The model for iodine was thought to require the following features:

a) inclusion of a third (atomic) level to account for the fact that iodine readily predissociates via the D state when excited to the B state,

b) the effect of a Gaussian intensity distribution in the exciting beam,

c) the introduction of an inhomogeneous lineshape factor.

It is felt the last element is needed because at low pressure the Doppler/Lorentz ratio of widths is about 440 MHz/10MHz = 44, while at high pressure the ratio is about 440 MHz/2290 MHz = 0.19. Because the laser linewidth is greater than the iodine linewidth at all pressures used (homogeneous contribution) but the laser runs in discrete modes (inhomogeneous contribution), this effect may be present in a varying degree as conditions change.

The three-level system used to develop the rate equations employed in this work is shown in Fig. 15. In actual fact, because rotational relaxation in iodine in the excited state is rapid and fluorescence occurs to

many ground state vibrational levels, a five-level scheme may actually be needed to describe these effects. It is hoped, however, that the essential physics are included in the three-level model shown in Fig. 15.

On the basis of the three-level model being considered, the time dependent populations of levels 1 and 2 are given by the following two coupled rate equations

$$\frac{dN_2}{dt} = B_{12}I_\nu N_1 - (B_{12}I_\nu + A_{21} + Q)N_2$$

$$\frac{dN_1}{dt} = -B_{12}I_\nu N_1 + (A_{21} + B_{21}I_\nu)N_2 + R(N_{atomic})$$

Using atom conservation

$$N_1 + N_2 + (N_{atomic})/2 = N_{total} ,$$

assuming steady state, and solving for N_2 with the introduction of detailed balancing ($g_1B_{12} = g_2B_{21}$), we obtain

$$N_2 = \beta N_{total} I_\nu/(I_\nu + I_\nu^{sat}) ,$$

where

$$\beta = \left[\frac{Q}{2R} + \frac{1}{2} + \frac{g_1}{g_2} \right]^{-1} \quad \text{and} \quad I_\nu^{sat} = \beta(Q + A_{21})/B_{12} .$$

Thus, the factor β now depends on the buffer gas pressure throught the ratio Q/R, as opposed to the constant that appears in Daily's two-level model.

On including the effect of a Gaussian intensity distribution across the laser beam, we obtain a result similar to Daily's given by

$$S = A \ln(1 + \tilde{I}) , \qquad (7)$$

where

$$A = h\nu \frac{A_{21}}{4\pi} \Omega_c \delta N_{total} \pi\omega^2 \beta \qquad \text{and} \qquad \tilde{I} = I_\nu / I_\nu^{sat}.$$

In the present model two parameters (A, I_ν^{sat}) depend on the total gas density or pressure, either directly through the term N_{total} or through the unknown rates Q and R. Because the two rates Q and R must account for a collection of different rates in the iodine molecule, and therefore they do not obey simple laws, we may use them as ajustable parameters in fitting the theory to the experimental data.

Before introducing the third element into the model which accounts for the lineshape, it is useful to analyze the saturation data on the basis of the present model and assume that A and I_ν^{sat} are the adjustable parameters and fit the theory to the data. A nonlinear least square fitting routine using a gradient search technique and two parameters was employed to fit the data. The main conclusions drawn were that the saturation intensity obtained in this way was not a monotonically increasing function of pressure and that the logarithmic function seemed to overcorrect the data at high intensity. Thus, the model needs to account for the variable lineshape.

Piepmeier's[6] analysis allows for the inclusion of a lineshape parameter but not for the Gaussian beam effect, and it applies only to the case of a narrow laser linewidth. Daily's analysis applies to the broadband laser case and can be made to include the Gaussian beam effect, but it is completely homogeneous. However, a lineshape parameter was added to Daily's model in the following way. In the homogeneous limit we find

$$S \sim \tilde{I}/(1 + \tilde{I}) ,$$

and in the inhomogeneous limit we have

$$S \sim \tilde{I}/(1 + \tilde{I})^{0.5} .$$

Consequently, if we assume the intensity always varies as

$$S \sim \tilde{I}/(1 + \tilde{I})^{\alpha} ,$$

then α becomes a lineshape parameter with the range $0.5 < \alpha < 1$. This approach is certainly not rigorous, because the full Voight profile integral would have to be done, but in light of the assumptions made it is felt to be a realistic approach.

Assuming the lineshape parameter α can be used in this way, the effect of the Gaussian intensity distribution across the beam can now be included as follows. The fluorescence signal, S, is obtained by integrating the upper state population, N_2, across a beam with an assumed Gaussian intensity distribution, i.e.

$$S = h\nu \frac{A_{21}}{4\pi} \Omega_c \int N_2 \delta 2\pi r \, dr ,$$

with

$$N_2 = \beta N_{total} (I_\nu / I_\nu^{sat}) / [1 + I_\nu / I_\nu^{sat}]^{\alpha}$$

$$I = I^o \exp(-r^2/\omega^2) .$$

This leads to the result

$$S = \frac{A}{(1-\alpha)} [(1 + \tilde{I})^{1-\alpha} - 1] , \qquad (8)$$

where A and $\tilde{I}$ have the same definitions as in (7).

It is easy to see that (8) reproduces the correct limits. We obtain the linear regime for $\tilde{I} \ll 1$, i.e.

$$S = A\tilde{I} ,$$

and for $\tilde{I} \gg 1$ the saturated result

$$S = \frac{A}{(1-\alpha)} [I^{1-\alpha} - 1] .$$

Using $\alpha = 1$ and L'Hospital's rule in the expression for the saturated limit, we recover the homogeneous saturated limit

$$S = A \ln \tilde{I} ,$$

and for $\alpha = 0.5$ the inhomogeneous saturated limit

$$S \sim \tilde{I}^{0.5} .$$

The theory now contains three adjustable parameters, the quenching rate Q, the recombination rate R, and the lineshape factor α, in the three constants A, α, and I_ν^{sat} which appear in (8). Again, it is far easier to allow A, α, and I_ν^{sat} to vary in a least squares fit of the saturation data and then to determine their mutual consistency afterwards. The theory was fitted to the saturation data for iodine in this way and the results are shown in Fig. 16 for the pressure range 200 torr to 800 torr nitrogen. Also shown are the values obtained for the three constants from the least squares fitting process as a function of nitrogen pressure.

The saturation intensity is now found to vary monotonically over the full range of pressures. Dividing by the 6 GHz Argon-ion laser bandwidth (0.2 cm^{-1}), gives in the limit of low pressure $I_\nu^{sat} = 4 \times 10^4$ Watts/$cm^2 cm^{-1}$

and for high pressure (800 torr) $I_\nu^{sat} = 1.75 \times 10^5$ Watts/cm^{2}cm^{-1}. These quantities can also be calculated in other ways from existing low-intensity quenching data. It is encouraging to find that the respective values agree rather well considering the fact that the two methods differ greatly.

The lineshape parameter α was found to vary smoothly from about 0.55 to 0.98, which is entirely consistent with its original introduction into the theory. The behavior of the lineshape parameter probably lends the strongest support for accepting the theory as a useful representation of the saturation process in iodine.

The parameter A varied smoothly from 10 at low pressure to 2 at high pressure. This parameter has less direct physical interpretation and one can only check its internal consistency. We have not completed this step in detail but it too appears to be quite consistent on the basis of a few rough calculations.

4. DENSITY MEASUREMENT

The data of Fig. 16 together with the proposed theory provide one with the necessary information to evaluate the first partial derivative appearing in equation (2), which expresses the sensitivity of a density measurement, using partially saturated fluorescence. A cross-plot of the data found in Fig. 16 is presented in Fig. 17, where the fluorescence signal (photomultiplier output in millivolts) is displayed versus the gas pressure (nitrogen) for three levels of the laser excitation intensity. The lines drawn in the figure are visual interpolations of the experimental data. We have also considered using equation (8), together with the pressure dependency found for the quantities A, α, and I_ν^{sat}, to obtain a curve fit for the region of pressure for which we do not have experimental data. However, our first efforts in carrying out these calculations have led to significant numerical errors, since it is difficult to find simple algebraic functions that will accurately represent the pressure dependency of the three quantities over the full range of pressure (0 to 10^3 torr).

By measuring the slope at a point on one of the curves in Fig. 17, one is able to obtain the partial derivative, $\partial S/\partial p$, directly, and this derivative corresponds to holding temperature, as well as laser intensity, fixed. Recalling that the first partial derivative on the right-hand side of equation (2) is also evaluated while holding temperature and laser intensity fixed, then for this case we may use the substitution

$$\frac{\rho}{S}\frac{\partial S}{\partial \rho} = \frac{p}{S}\frac{\partial S}{\partial p} \quad . \tag{9}$$

Because the data in Fig. 17 appear on a log-log scale, the dimensionless

derivative in (9) is given directly by the tangent of the slope at a point in the figure. In the range of pressures above 50 torr where gas dynamic experiments would normally be carried out, this number is essentially -1 for all levels of laser excitation intensity used in the experiment. Therefore the -1 cancels the +1 appearing in equation (2), and one is left with only the third term in the expression. This is the same situation one faces for the unsaturated condition. It is clear that although partial saturation is apparent in Fig. 16, this does not significantly affect the slope in Fig. 17 due to the three-level effect in iodine. Thus, saturation of fluorescence in iodine does not aid in improving the sensitivity of the density measurement scheme.

Because there is reason to believe that the second partial derivative in equation (2) is relatively small, we have not conducted any experiments to measure it directly and thereby obtain a complete measure of the magnitude of the coupling coefficient in (2). However, we have indirect evidence that leads us to suspect that it is small and that the coupling coefficient in (2) cannot be near 1. The indirect evidence is based on some iodine saturation data that we have collected using a small supersonic free-jet nozzle. The flow in the nozzle was seeded with iodine at the vapor pressure for room temperature and the flow was expanded in the free jet to a Mach number of about 5 where the temperature of the gas was near 50 K. The fluorescence intensity was measured along the axis of the jet and found to be nearly constant. This leads one to believe that the second partial derivative in (2) must be small because we have already found that the first partial derivative in (2) essentially cancels the +1, and this cancellation would result in a constant fluorescence signal.

The study to this point shows that atempts to saturate iodine for the pressure levels of interest in gas dynamic experiments have not led to a significant value for the coupling coeficient in the density measurement scheme being explored. However, the principal concept we are pursuing is embodied in equation (2), and we are interested in all methods that may lead to a finite value of the coupling coeficient. Saturation is only one of several ways this could be achieved.

There has been much discussion in the literature about the difference between fluorescence and resonant Raman scattering. The currently accepted point of view is that they are variations of the same physical process, distinguished by the amount of detuning from the line center of the transition. Off line center the process is nearly instantaneous Raman scattering (10^{-12} sec or less), insensitive to quenching. Fluorescence is the much larger signal occuring when tuned within an absorption linewidth. In this case the scattering time becomes the lifetime of the transition, which is usually much larger than 10^{-12} sec and, thus, subject to quenching. Williams et al.[7] excited iodine in a cell with 100 nsec laser pulses and measured the decay time of the emitted photons at different excitation wavelengths. They showed that on line center the decay time was about 10^{-6} sec, characteristic of fluorescence, and by detuning more than 1.6 GHz the decay time was reduced to less than 10^{-8} sec, the temporal resolution for their experiment.

Using this point of view, one has the option of trading signal amplitude for a significant decrease in the effects of quenching. We have conducted a preliminary experiment in iodine employing the concept of resonant Raman scattering. These results are shown in Fig. 18 and were

obtained using a Q-switched ND:YAG laser running at 10 pulses per second and frequency doubled to 532 nm. The output was line narrowed by an intracavity etalon and was tunable over about 3 cm^{-1} (90 GHz) by tilting the etalon. The fluorescence data were obtained with the ND:YAG laser tuned onto the line center of a strong and relatively isolated iodine transition. The resonant Raman scattering data correspond to approximately 6 GHz detuning off this transition. The fluorescence data differ from that shown in Fig. 17 because of the short pulse length (<10 nsec) excitation of the Q-switched ND:YAG laser and the resulting partial saturation that is achieved with it. The figure shows that the resonant Raman signal is nearly independent of nitrogen gas pressure up to an atmosphere of pressure. An equally important observation is the fact that the level of the resonant Raman signal corresponds to the level of the fluorescent signal at atmospheric pressure. These two facts make it reasonable to reconsider the application of equation (2) by employing resonant Raman scattering in iodine to develop an acceptable value for the coupling coefficient in the density measurement scheme.

Our general approach in studying the problem of density measurement through the use of laser-induced fluorescence or, more generally, resonantly enhanced scattering, can be described by the use of the schematic diagram in Fig. 19, together with equation (2). In the range of pressures of interest for gas dynamic studies, the fluorescence signal versus pressure falls off with a slope of -1 (due to quenching) and the resulting sensitivity from (2) is zero. Our first efforts were to attempt to saturate iodine in this range of pressures because this should lead to a reduction in the slope and an increased signal level, both highly desirable in

the desity measurement scheme. However, we found that saturation effects in iodine were not effective in producing the desired sensitivity. The alternative is to accept a somewhat lower signal level and employ resonant Raman scattering. As indicated in the figure, detuning leads to decreased slopes in the curve and, thus, to more sensitivity, but at the expense of signal level. Experiments are currently being performed in a supersonic free jet expansion to quantatatively evaluate the effects of detuning on signal level and sensitivity.

5. REFERENCES

1. "Iodine, A Test Molecule in Modern Spectroscopy," J.C. Lehman, Contemp. Physics, vol 19, no 5, p 229, (1978).
2. "Assignments of Several Groups of Iodine Lines in the B-X System," S. Gerstenkorn and P. Luc, Jour. Mole. Spectroscopy, 77, p 310 (1979).
3. "Saturation Effects in Laser Induced Fluorescence Spectroscopy," J.W. Daily, Applied Optics, vol 16, no 3, p 568, (1977).
4. "Linewidth and Tuning Effects in Resonant Excitation," H. Greenstein and C.W. Bates, Jr., Journal of the Optical Society of America, vol 65 no 1, p 33, (1975).
5. "Intensity and Pressure Dependence of Resonance Fluorescence of OH Induced by a Tunable UV Laser," D.K. Killinger, C.C. Wang, M. Hanabusa Phys Review A, vol 13, no 6, p 2145, (1976).
6. "Theory of Laser-Saturated Atomic Resonance Fluorescence," E.H. Piepmeier, Spectrochimica Acta, 27B, p 431, (1972).
7. "Resonant Fluorescence and Resonant Raman Scattering: Lifetimes in Molecular Iodine," P.F. Williams, D.L. Rosseau, S.H. Dworetsky, Phys Review Letters, vol 32, no 5, p 196, (1974).

6. PERSONNEL

Professor D. Baganoff

The subject has been of interest to Prof. Baganoff for a number of years and his participation has provided program continuity and direction, and has involved a regular review and study of specific problems associated with the project.

J.C. McDaniel

Mr. McDaniel, an advanced Ph. D. candidate in the Department of Aeronautics and Astronautics, has been the Research Assistant on the project since its inception, and his research represents a major portion of the work supported by the grant. Most of his experimental work was carried out in Prof. Byer's laboratory in Applied Physics, who's generous assistance in providing laboratory facilities and technical advice has been invaluable to the progress of the study.

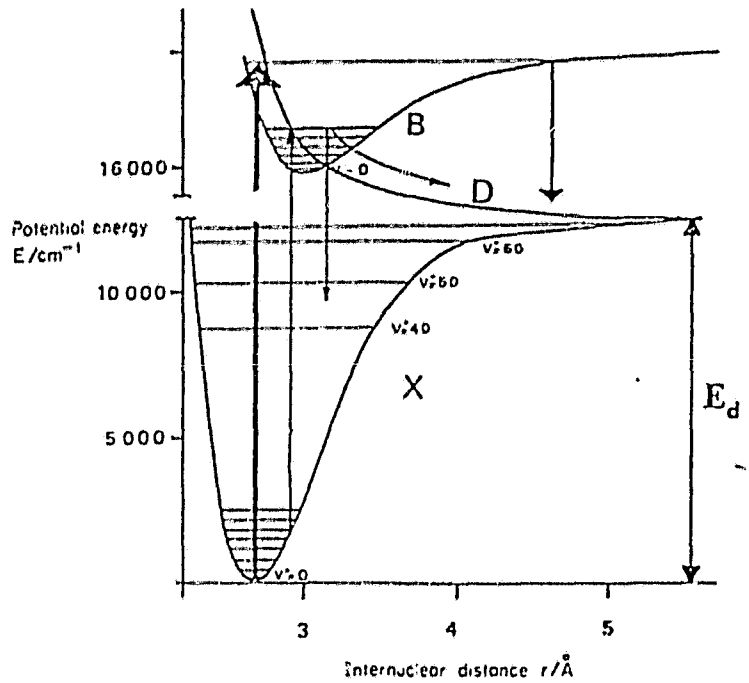

Fig. 1 Potential energy curves of the X and B states of molecular iodine. r is the internuclear distance. Also shown is the curve of the dissociative D state.

(FROM REF. 1)

FIGURE 2. IODINE SPECTRAL ASSIGNMENTS NEAR 514.5 Å (FROM REF. 2)

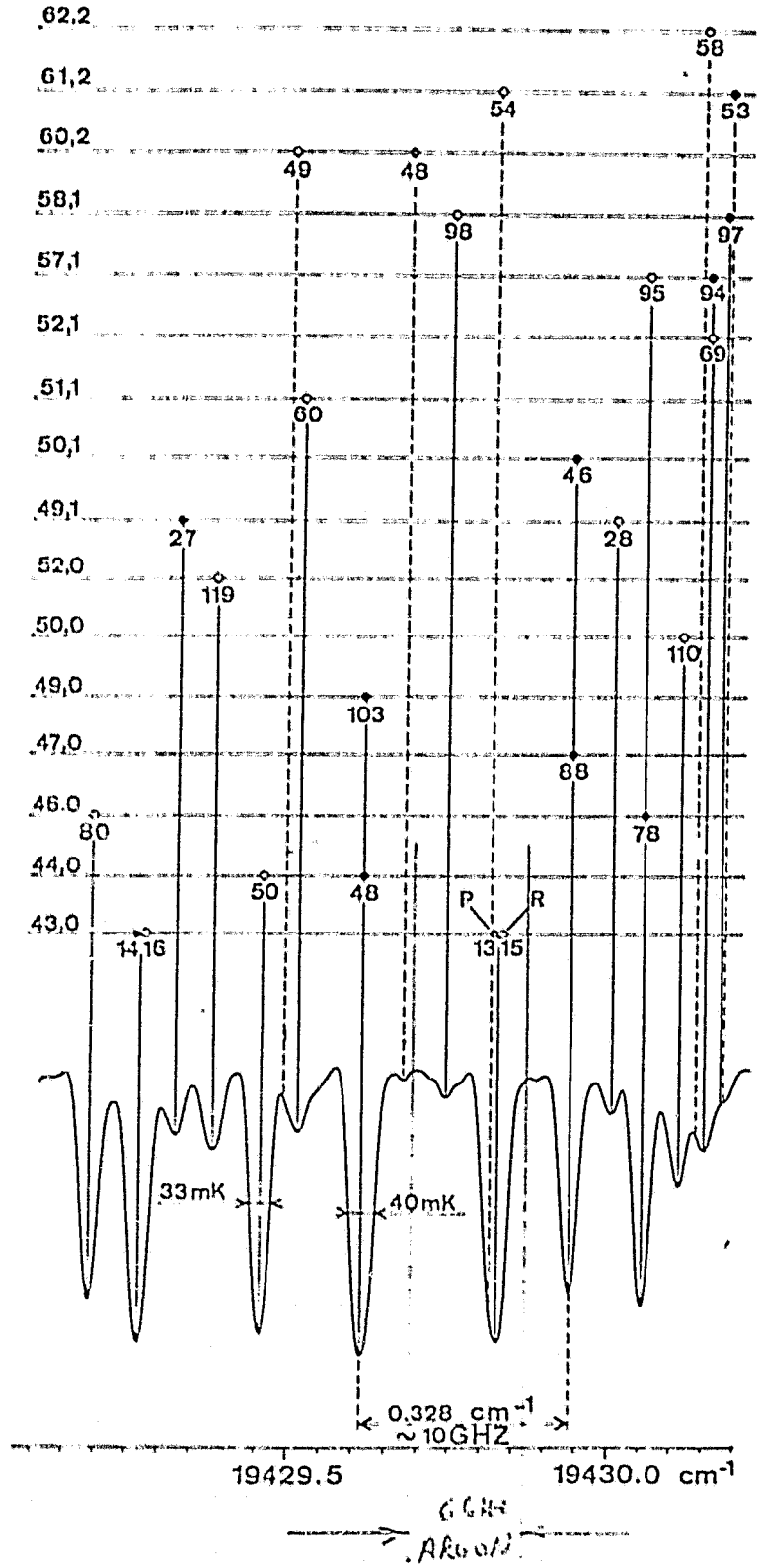

FIGURE 3. n^{th} STOKES BAND FLUORESCENCE RESULTING FROM P12, R15 ABSORPTION LINES

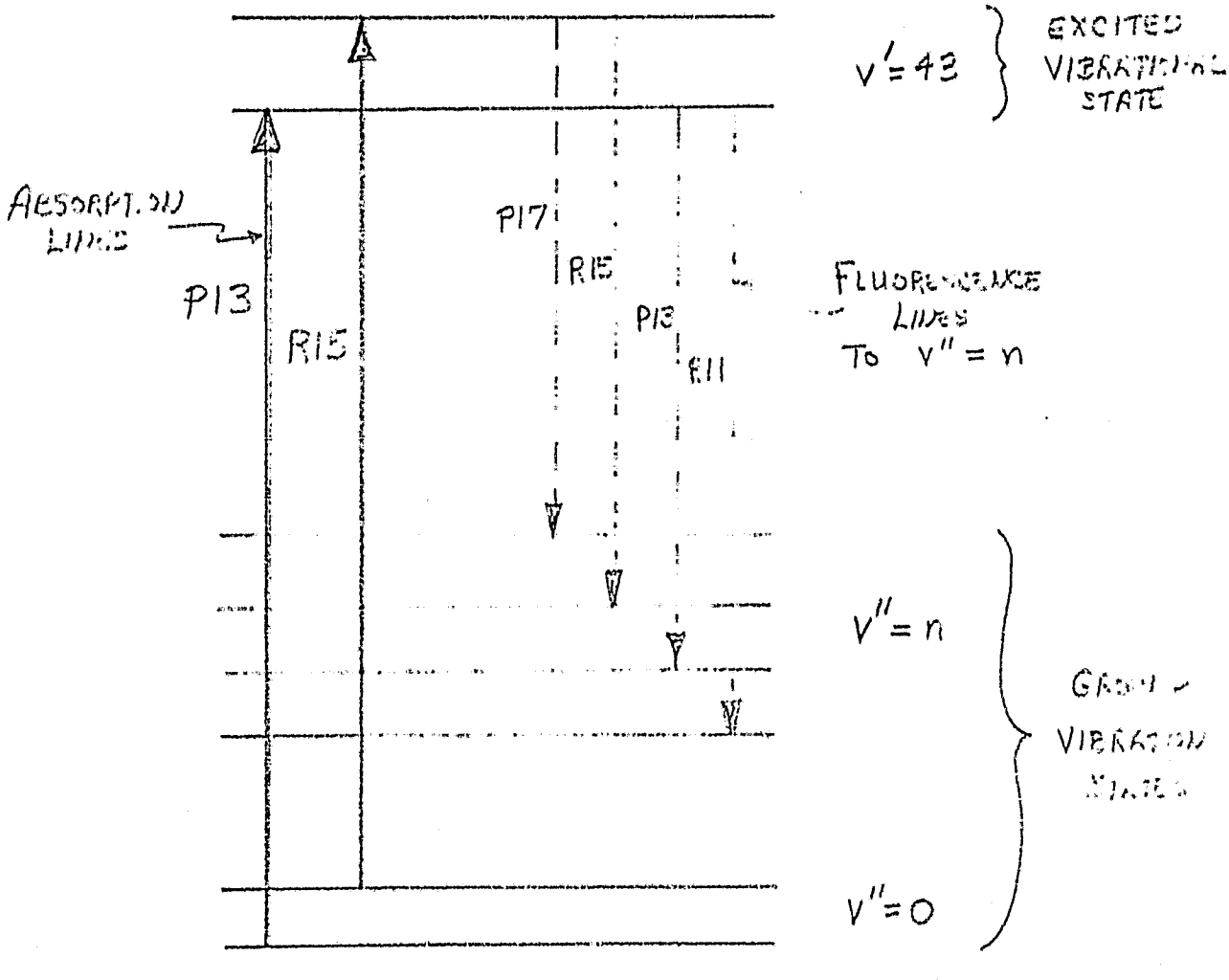

FIGURE 4: FLUORESCENCE FROM LOW PRESSURE I_2 CELL

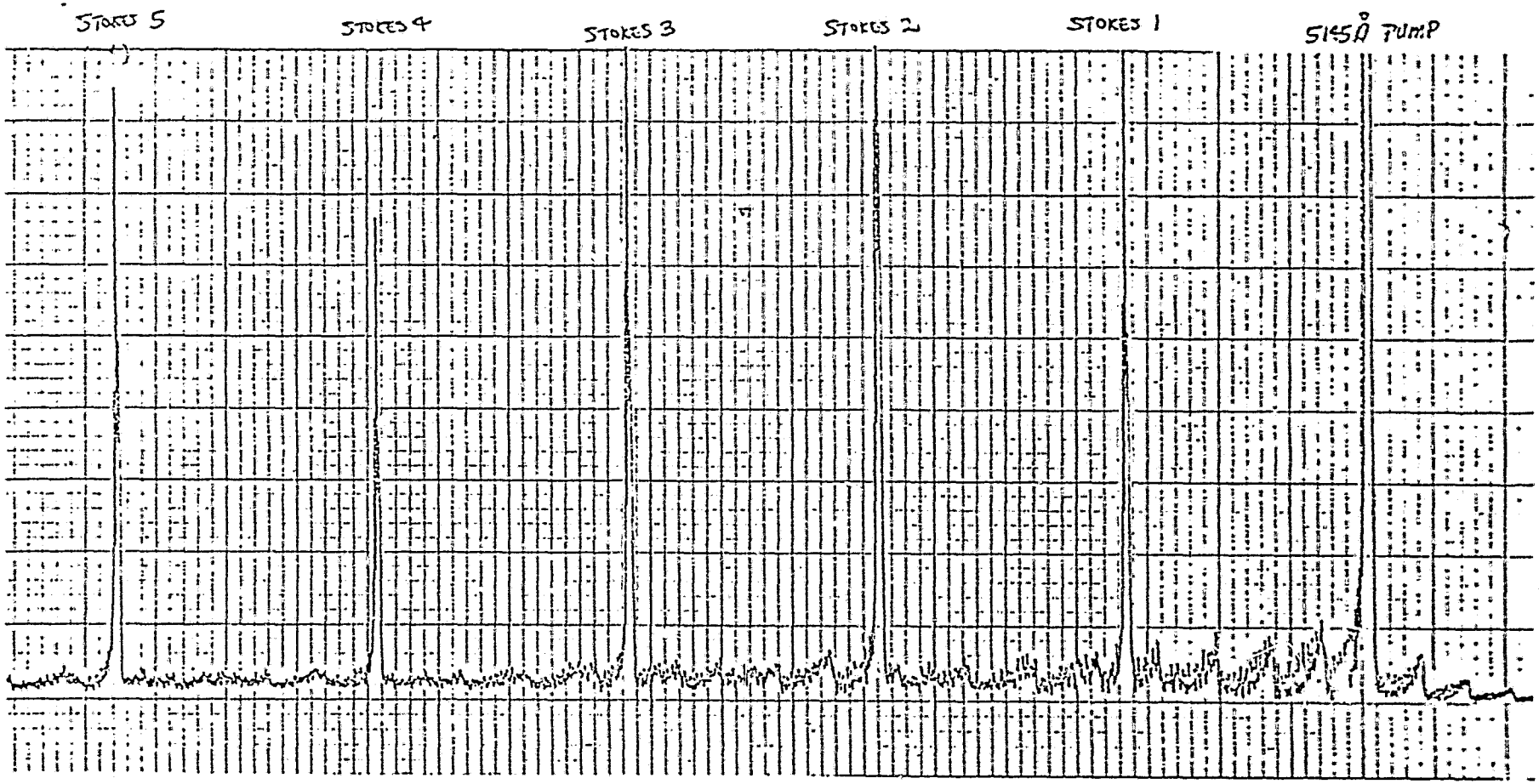

FIGURE 5: TRIPLET STRUCTURE OF 2nd STOKES VIBRATIONAL BAND AT 5260 Å

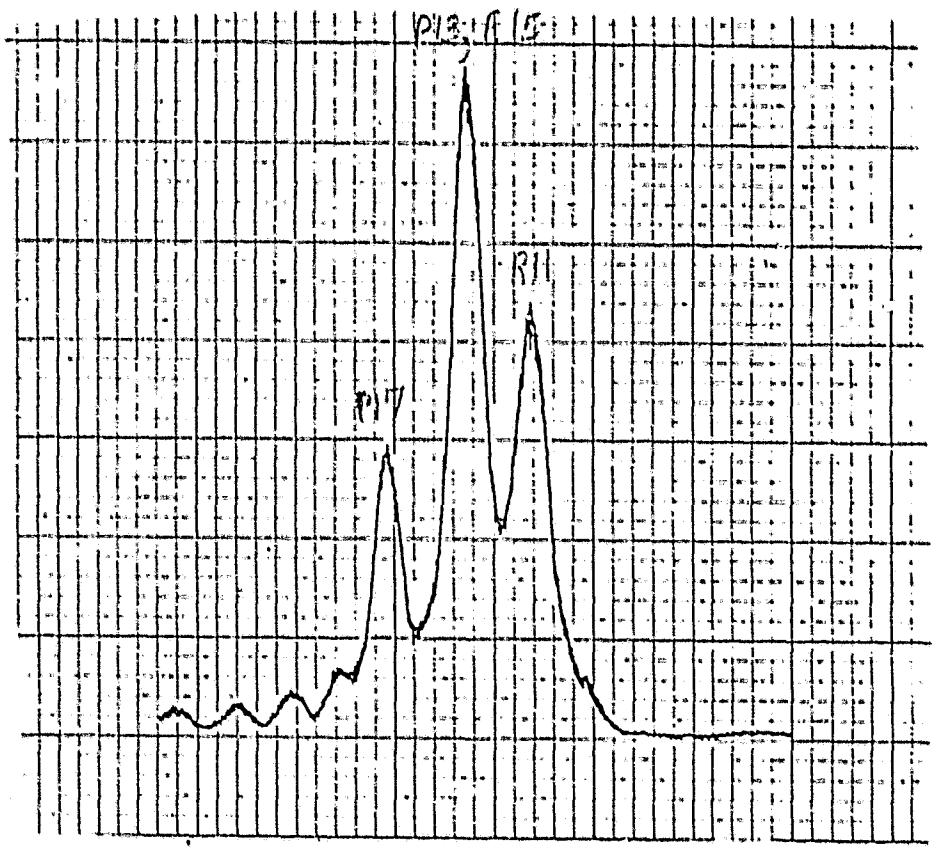

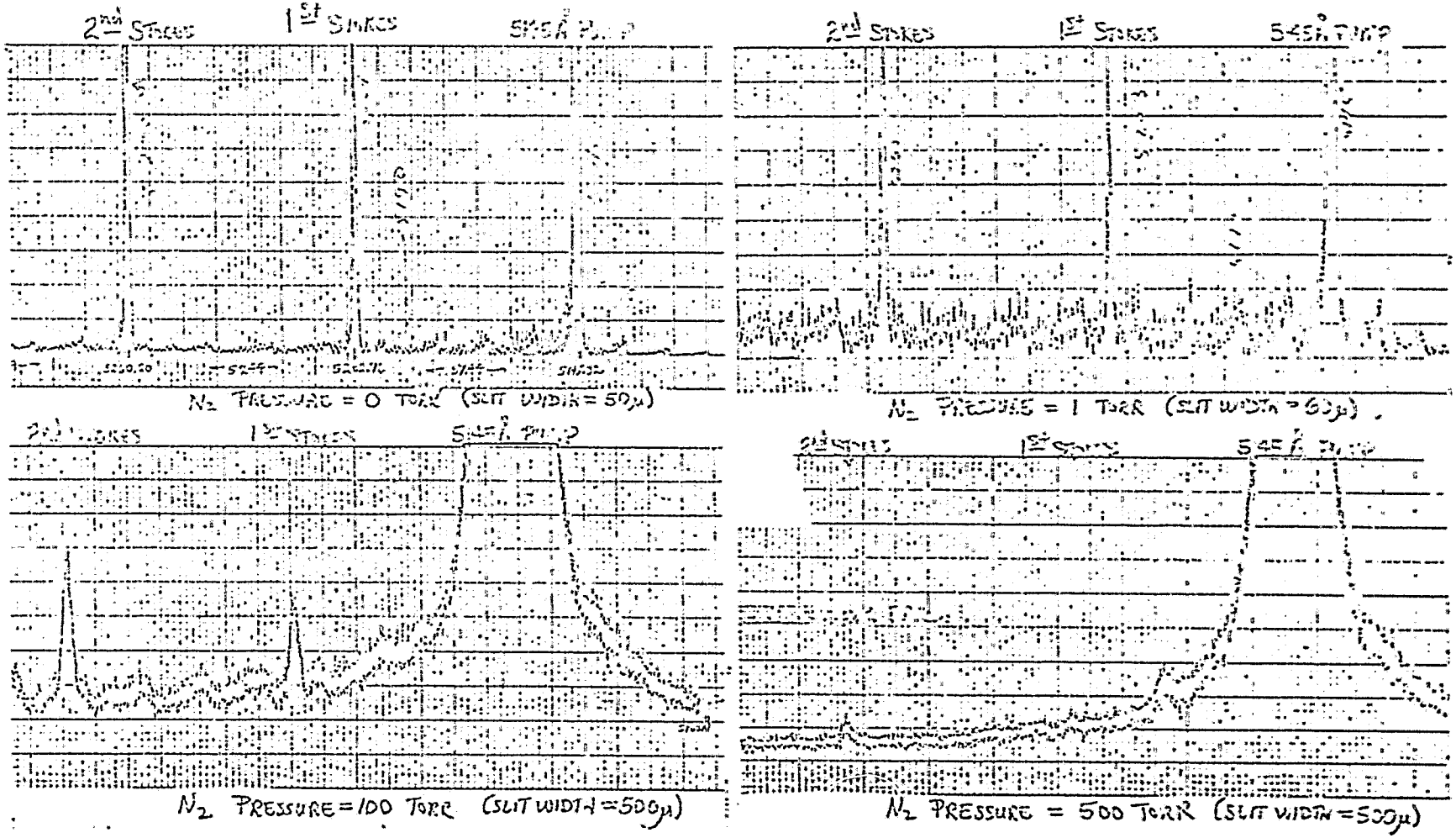

FIGURE 6. IODINE FLUORESCENCE SPECTRUM AT FOUR NITROGEN BUFFER PRESSURES

FIGURE 7. EXPERIMENTAL SETUP, IODINE SATURATION

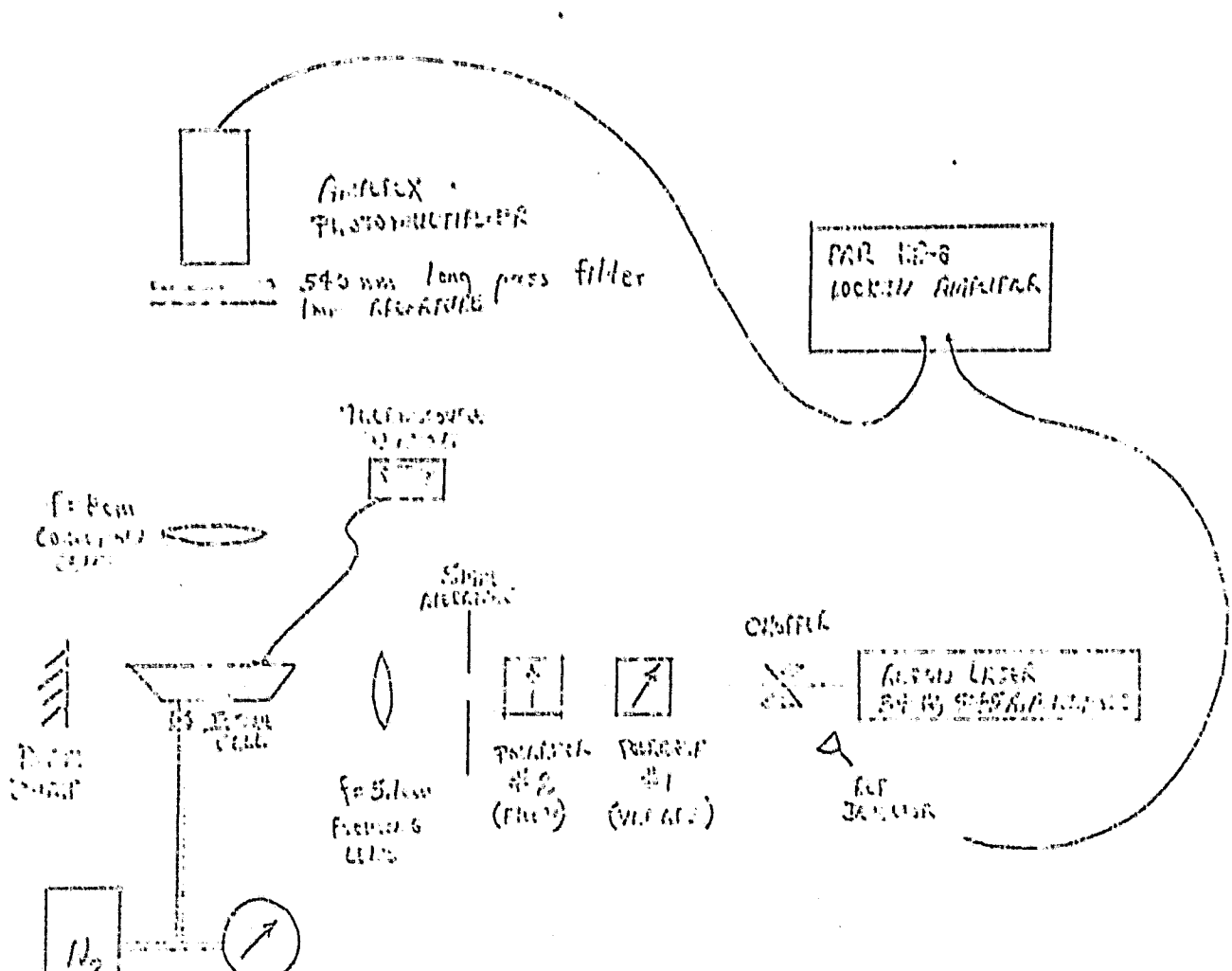

K&E LOGARITHMIC 46 7522
3 X 3 CYCLES MADE IN U.S.A.
KEUFFEL & ESSER CO.

FIGURE 8 : SATURATION OF I_2 IN 0.9 TORR N_2

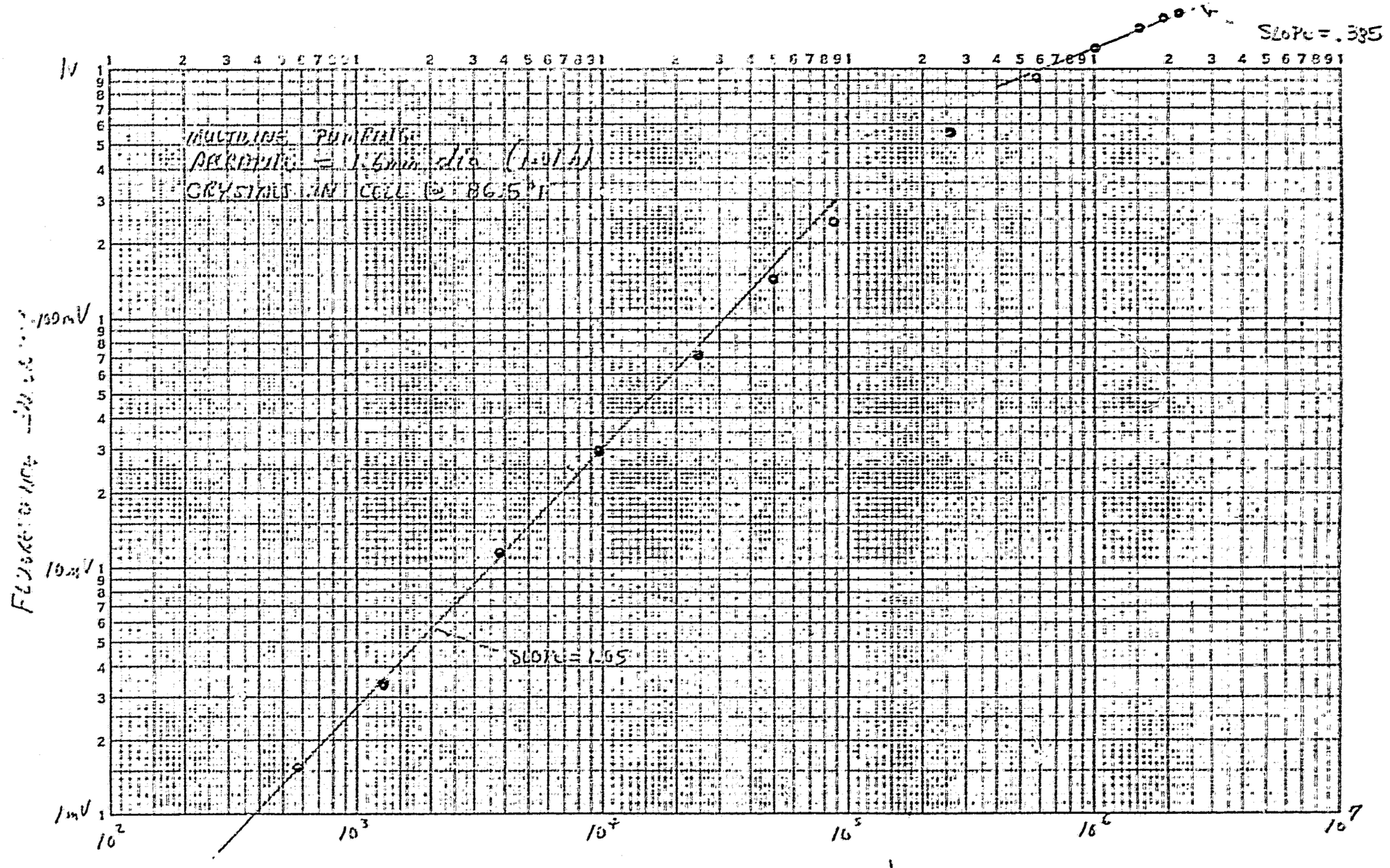

7/29/80

K&E LOGARITHMIC 46 7522
3 X 5 CYCLES MADE IN U.S.A.
KEUFFEL & ESSER CO.

FIGURE 9 : SATURATION OF I_2 IN 50 TORR N_2

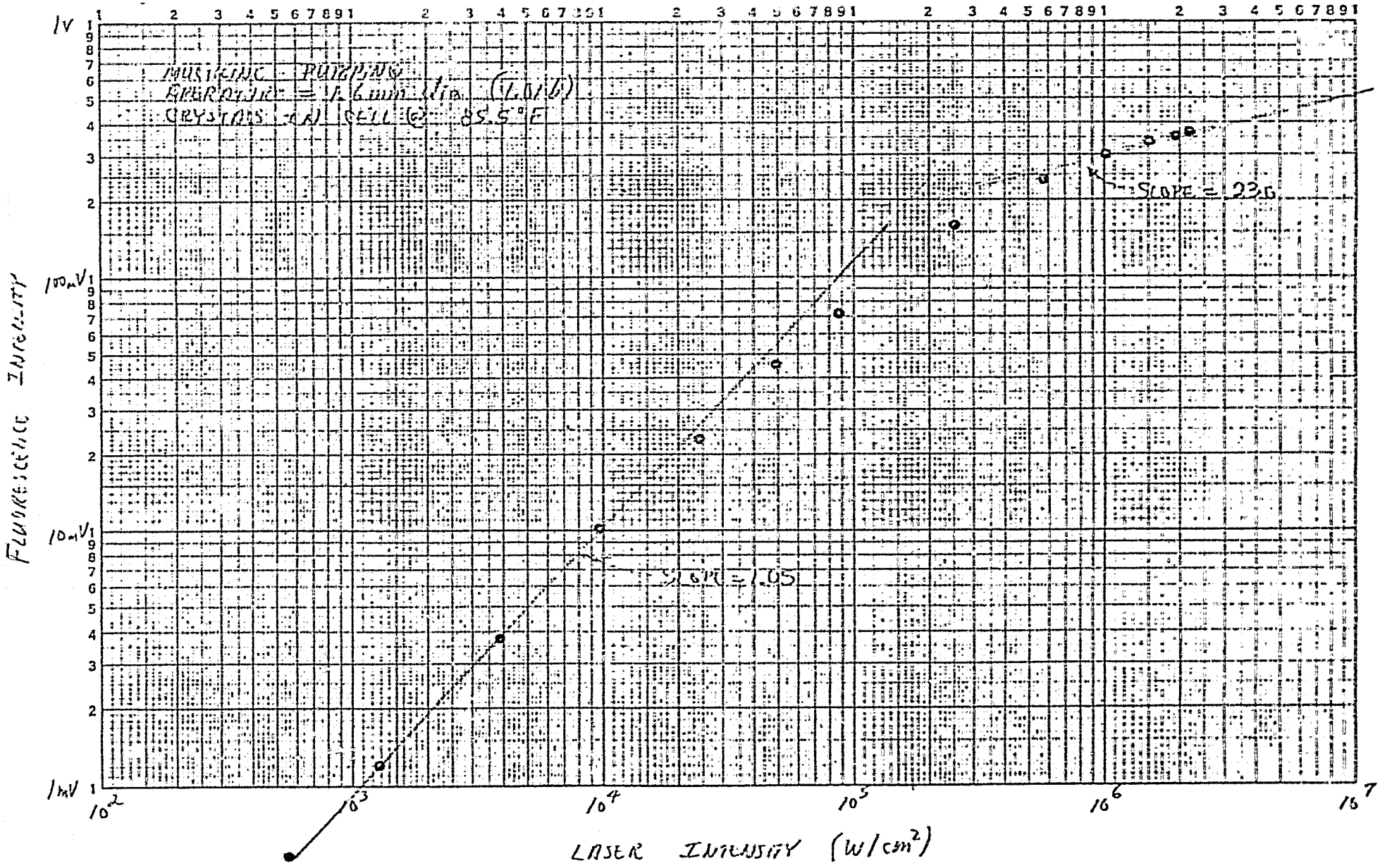

7/29 0

FIGURE 10: SATURATION OF I_2 IN 100 TORR N_2

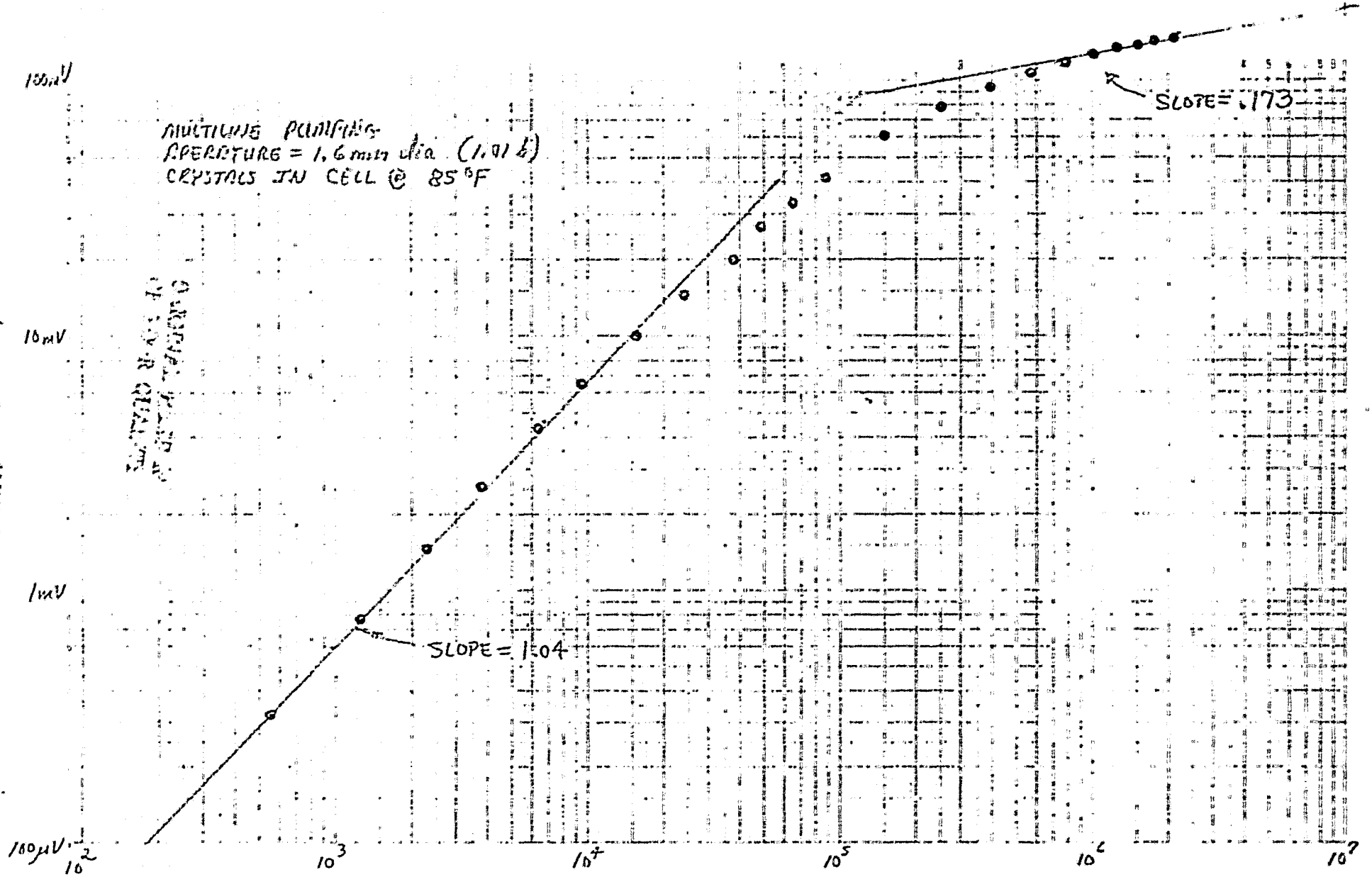

FIGURE 11: SATURATION OF I_2 IN 200 TORR H_2

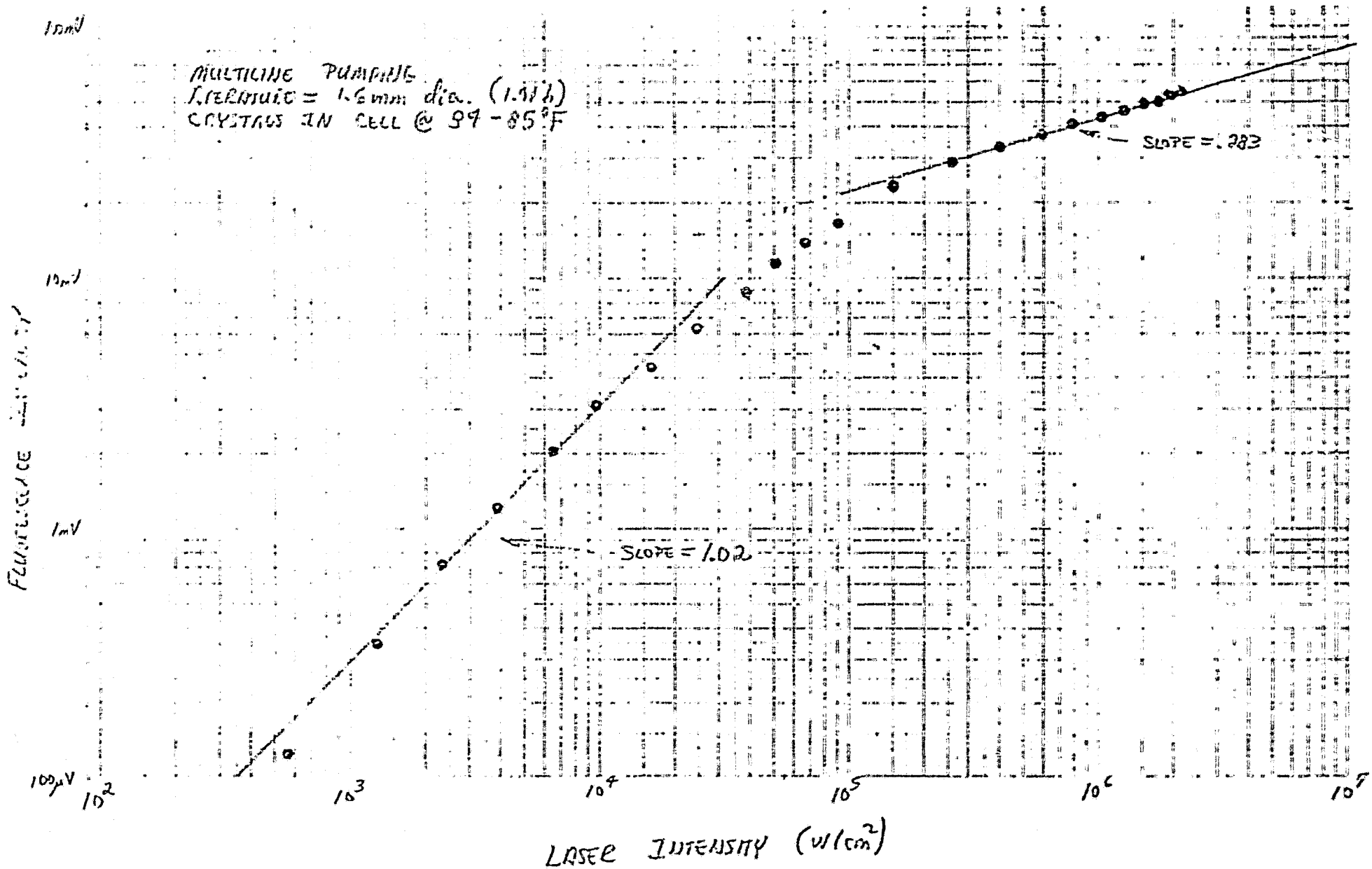

7/2./80

FIGURE 12: SATURATION OF I_2 IN 400 TORR H_2

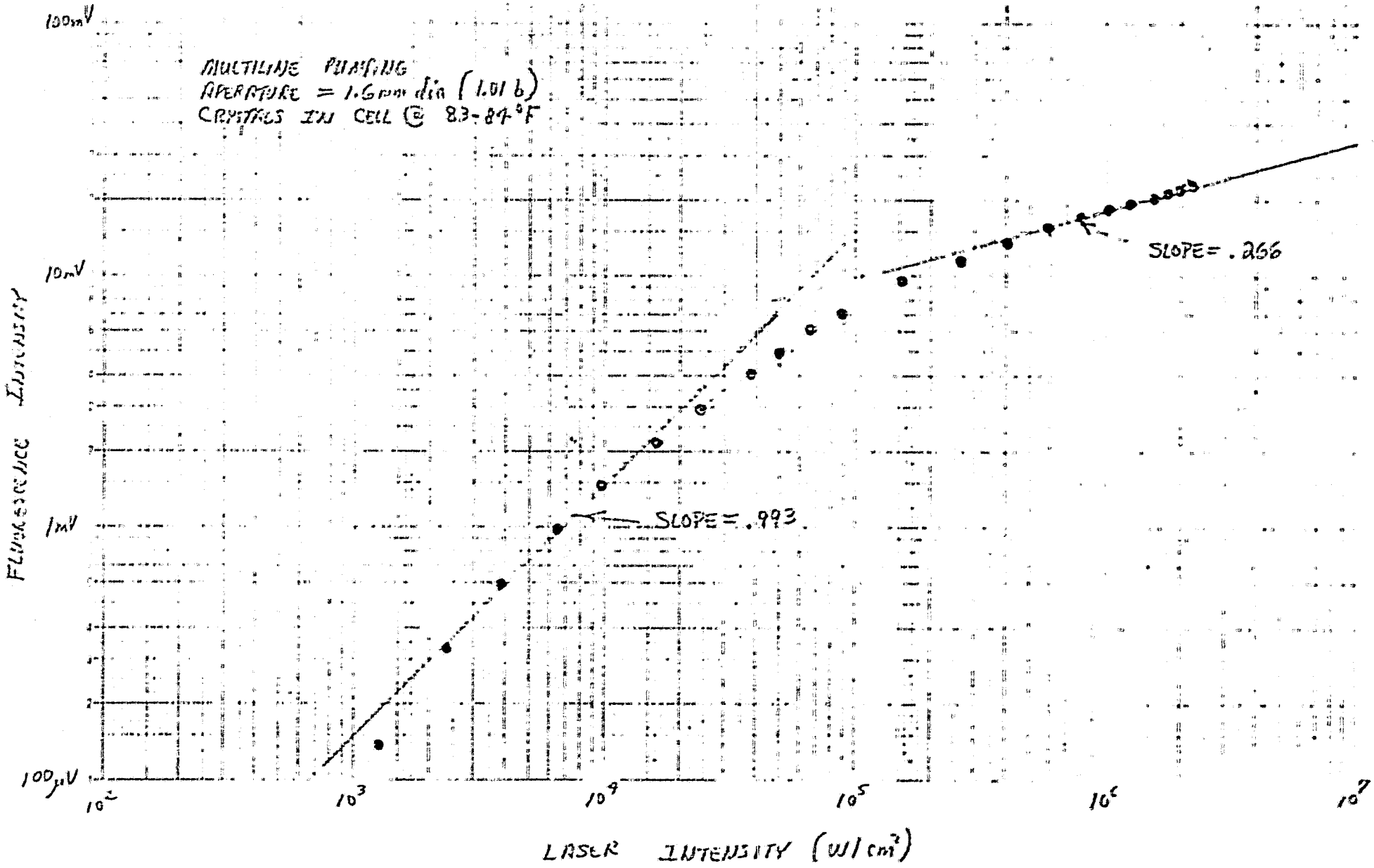

FIGURE 13: SATURATION OF I_2 IN 600 TORR N_2

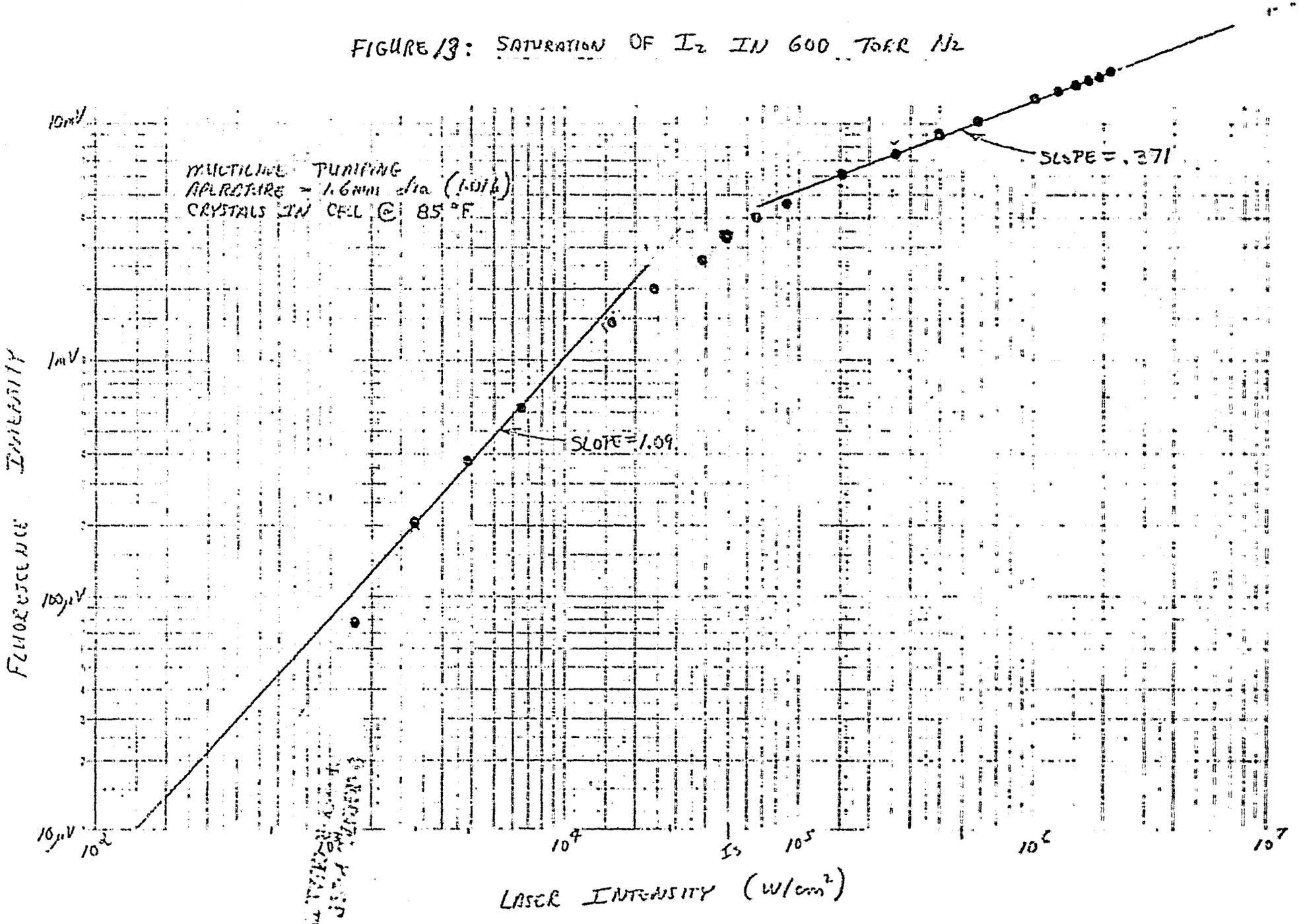

7/11/80

FIGURE 87: SATURATION OF I_2 IN 800 TORR N_2

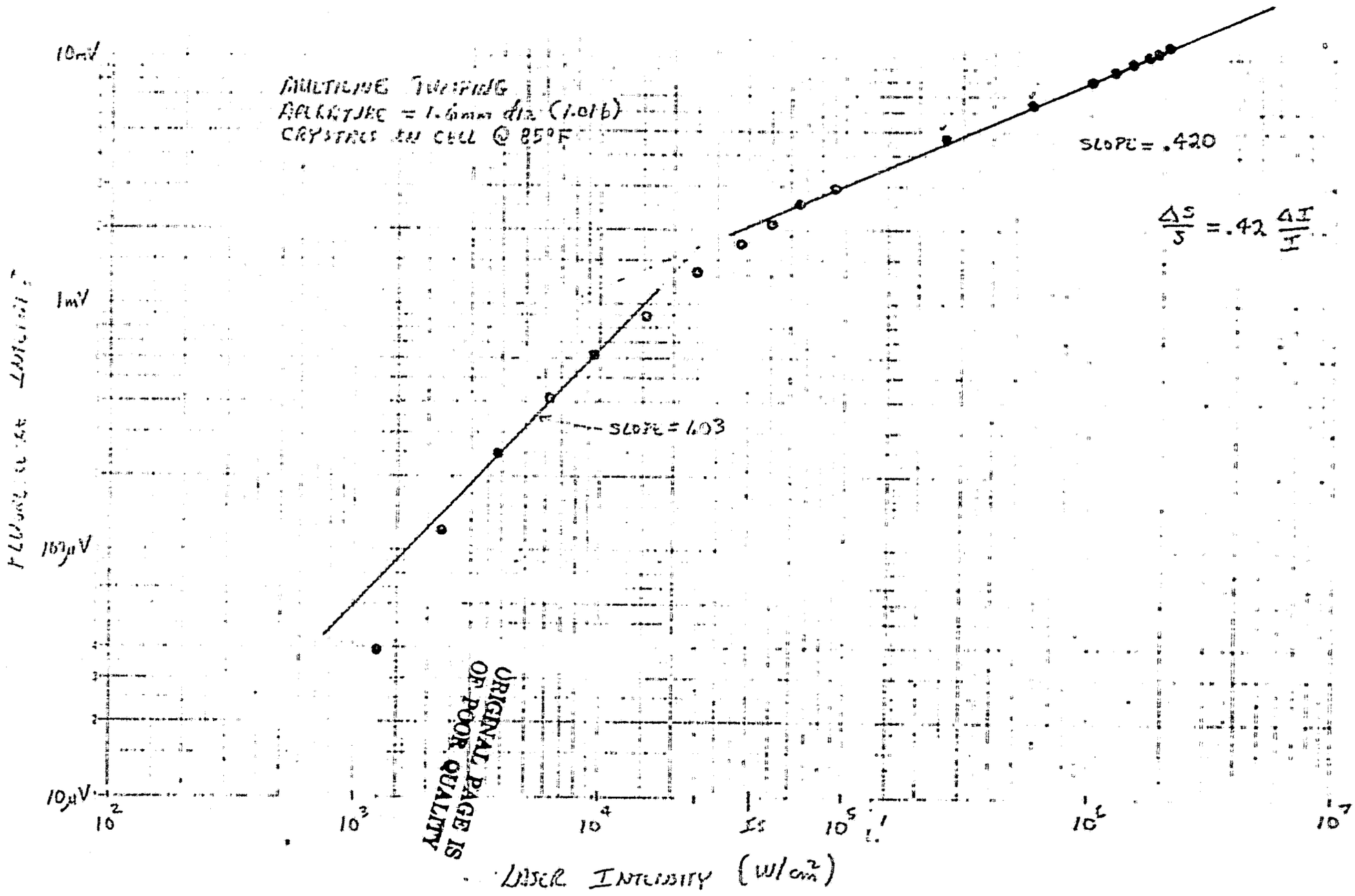

1/29/80

Fig. 15:

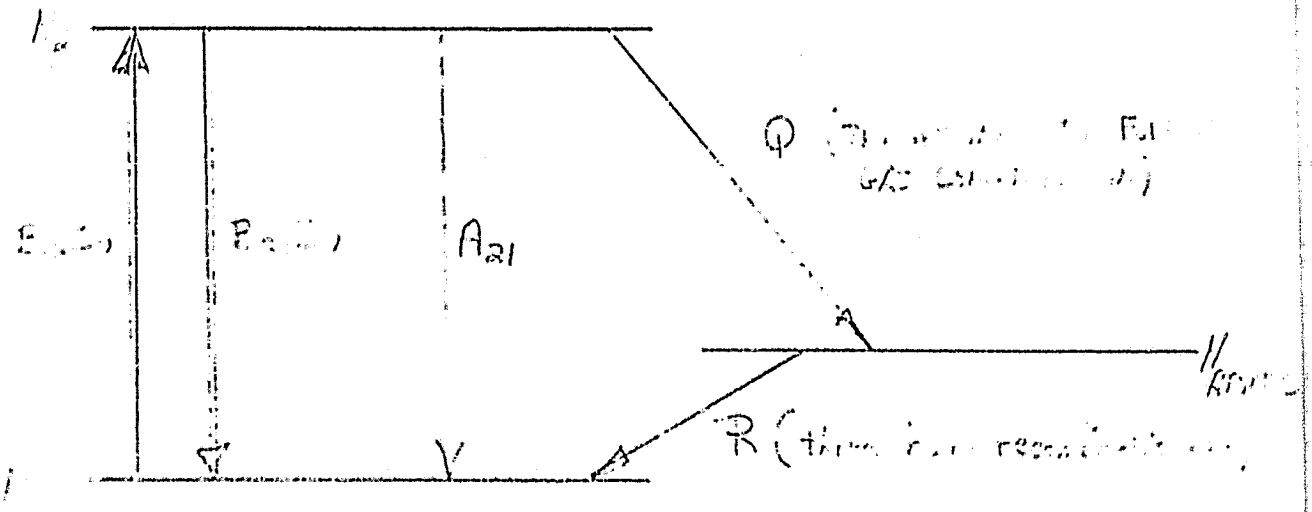

FIGURE 16. IODINE SATURATION FROM TWO THREE PARAMETER CURVE FITS

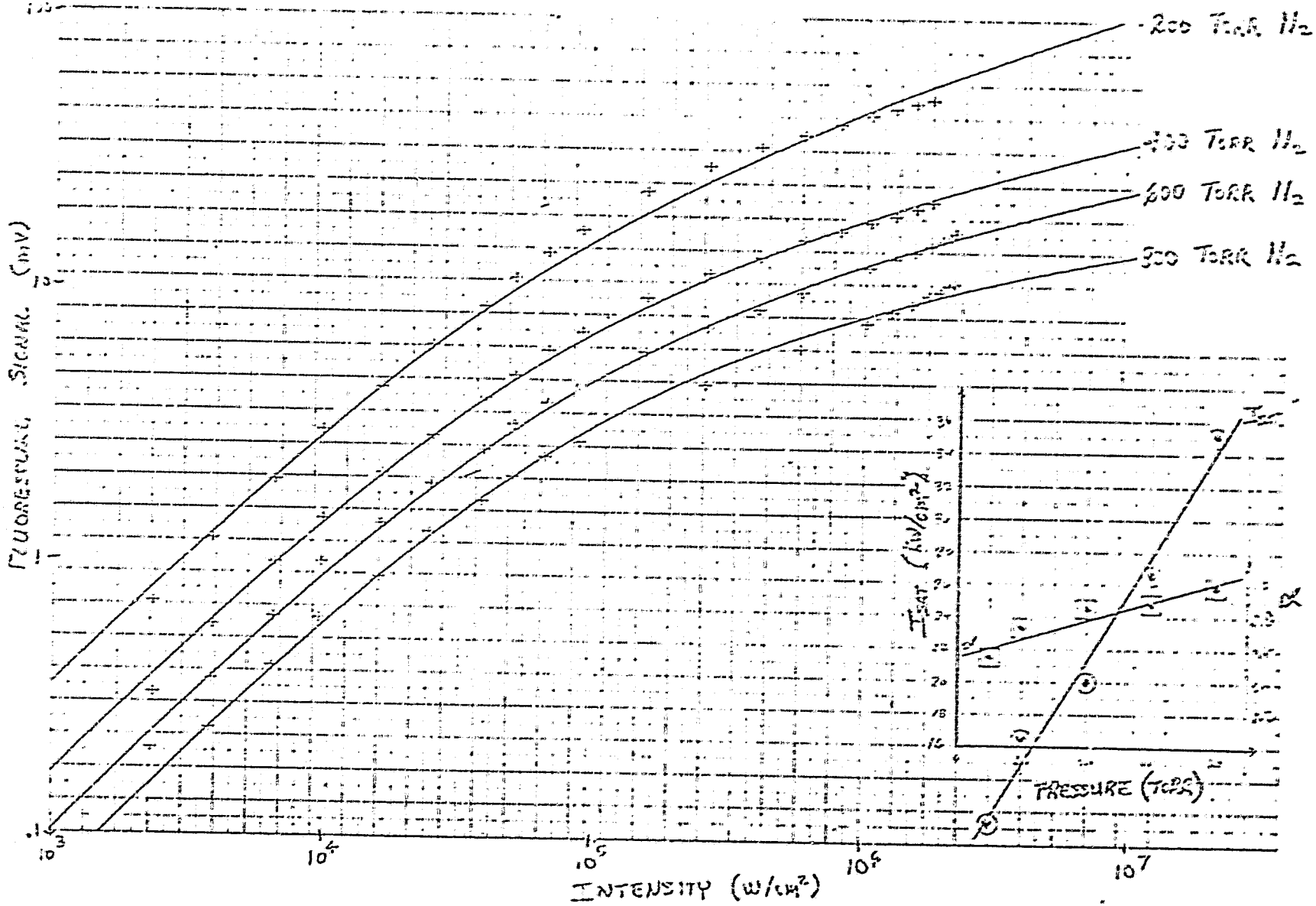

LASER INTENSITY
10^{8} QUANTS/cm^2
6.7×10^{-4}
2.5×10^{-3}
FLUORESCENCE SIGNAL
10^{3}
10^{2}
10
1
1
10
10^{2}
10^{3}

FIGURE 18. SCATTERING SIGNAL FROM IODINE AT 2nd STOKES VS N_2 BUFFER PRESSURE, USING 532nm LASER PULSES